Available online at www.sciencedirect.com
ScienceDirect
Sensors and Actuators A 142 (2008) 263–269
SENSORS AND ACTUATORS A PHYSICAL
www.elsevier.com/locate/sna

Power MEMS—A capacitive vibration-to-electrical energy converter with built-in voltage

Ingo Kuehne [a,*], Alexander Frey [a], Djordje Marinkovic [a], Gerald Eckstein [a], Helmut Seidel [b]

[a] *Siemens AG, Corporate Technology, Otto-Hahn-Ring 6, 81739 Munich, Germany*
[b] *Saarland University, Chair of Micromechanics, Microfluidics/Microactuators, Postfach 15 11 50, 66041 Saarbruecken, Germany*

Received 28 September 2006; received in revised form 22 December 2006; accepted 25 February 2007
Available online 7 March 2007

Abstract

This paper reports on the design and analysis of a capacitive vibration-to-electrical energy converter. A theoretical design model of a parallel-plate electrostatic spring-mass-system is presented, based on state space equations. The charging of the parallel-plate capacitor takes place by utilizing materials with different work functions for the electrodes. Numerical simulations are performed in order to optimize design parameters targeting a maximum output power. The shown Micro-Electro-Mechanical System (MEMS) based capacitive energy converter is able to provide an output power of 4.28 μW at an external vibration with a frequency of 1 kHz and an amplitude of 1.96 m/s^2 (0.2 g). A basic electronic circuit for storing the electrical energy is also introduced. Furthermore, a MEMS design and a process flow are presented.

Keywords: Power MEMS; Energy converter; Capacitive energy conversion; Vibration-to-electrical conversion; Built-in voltage

1. Introduction

The development of energy autonomous microsystems enables entirely new fields of applications especially in the range of wireless and maintenance-free sensor nodes. These microsystems are powered by electrical energy generated from the environment, e.g. vibration, heat, radiation, pressure variations or chemical energy. For instance, a wireless smoke detector for room monitoring in buildings consumes about 1.2 μW and a combination of a wireless temperature and pressure sensor for automotive applications requires about 3.8 μW of electrical power in average [1]. This amount of electrical power can be provided by the capacitive vibration-to-electrical energy converter especially for higher frequency applications in the range of 500 Hz to 10 kHz. Appropriate applications for microsystems including this particular energy converter are for example monitoring three-phase motors [2] and switched reluctance motors [3], because of their relatively wide vibration spectra with significant mechanical resonances in the higher frequency range.

There are three widespread physical principles for vibration-to-electrical energy conversion—piezoelectric [4–7], capacitive [8,9] and inductive [10–13]. The capacitive principle can be implemented with particular ease in MEMS technology. A charged parallel-plate capacitor arranged as a spring-mass-system converts mechanical energy into electrical energy. The capacitive principle requires the charging of the capacitor at all times to assure the conversion. This can be realized by charging the capacitor with a dedicated electronic circuit [14]. This approach has the disadvantages of an additional complex circuitry and relatively high electrical losses. Another way of biasing the capacitor is using an electret [15,16]. In this case the technology causes high costs due to the production and the poling of the dielectric electret material. Electrets are also known for problems regarding long-term stability. This paper reports on a different approach to charge the parallel-plate capacitor making use of the difference in work functions of two different materials. There is no need for an additional electronic circuitry and the MEMS technology involved is relatively simple compared to the electret concepts.

2. Theoretical design model

2.1. Design principle

The energy converter consists of a parallel-plate capacitor arranged as a spring-mass-system. Fig. 1 demonstrates the

* Corresponding author. Tel.: +49 89 636 41603; fax: +49 89 636 47630.
E-mail address: ingo.kuehne.ext@siemens.com (I. Kuehne).

0924-4247/$ – see front matter © 2007 Elsevier B.V. All rights reserved.
doi:10.1016/j.sna.2007.02.036

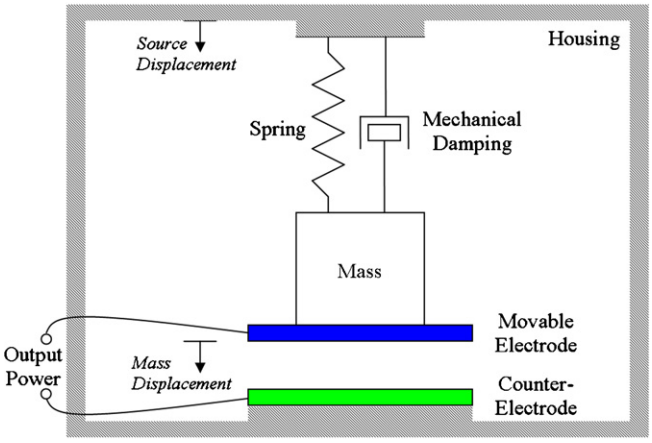

Fig. 1. Schematic design of the energy converter.

schematic design. The mass is both inertial mass and movable electrode of the variable capacitor. The housing of the converter includes the fixed counter-electrode and is coupled to an external vibration source. Doing so, the housing vibrates with the frequency and amplitude of the vibration source. Consequently, the inertial mass is forced to move periodically, but with a possible shift in amplitude and phase compared to the housing, depending on frequency and resonance phenomena. This results in a periodic and relative movement of the electrodes arranged in the parallel-plate capacitor. The changing width of the capacitor gap leads to a periodic change of the stored electrical energy assuming that the capacitor is charged.

2.2. Capacitor biasing

The movable electrode consists of a material (metal) with a work function ϕ_2. The counter-electrode is composed of a second material (metal) with a different work function ϕ_1. Both electrodes are aligned at vacuum level E_{Vacuum} as long as they are not brought into contact. As soon as the two electrodes are electrically contacted – e.g. via an external wire bond – the Fermi levels E_{Fermi} are equilibrated. Fig. 2 illustrates this behavior schematically. The equilibration of the Fermi levels requires an electronic current. Electrons originating from the material with the lower work function flow to the material with the higher work function. The electrode with the higher work function material is negatively charged and vice versa. Consequently, a contact potential difference V_{B} establishes between the electrodes. V_{B} is also referred to as contact voltage (or built-in voltage) and makes sure that the variable capacitor is charged as soon as the electrodes are electrically contacted.

An appropriate combination of materials has to be chosen so that the contact potential difference is maximized. Adequate materials are aluminum (Al) with $\phi_1 = 4.08\,\text{eV}$ and platinum (Pt) with $\phi_2 = 6.35\,\text{eV}$ [17]. This results in a contact voltage of $V_{\text{B}} = 2.27\,\text{V}$. Oxidized aluminum layers are reported to have work functions in the range of 10 eV. A corresponding combination of materials would actually lead to a higher contact voltage of approximately $V_{\text{B}} \approx 5\,\text{V}$.

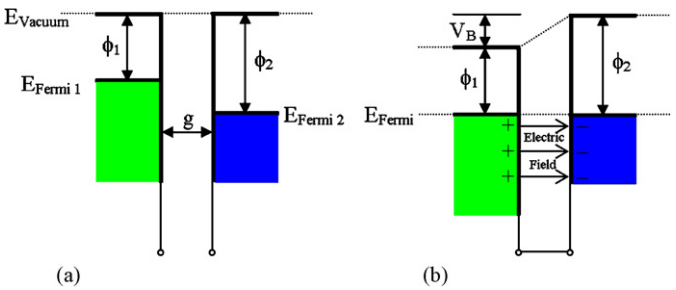

Fig. 2. Energy band-diagrams. (a) Before electrical contact and (b) after electrical contact.

2.3. Electrical load

The pure electrical part of the capacitive energy converter consists of a variable parallel-plate capacitor and a not really physically existing voltage source—V_{B} only represents the contact voltage. A simple external load (e.g. resistor) is connected to the converter to accomplish an equivalent circuit diagram which is shown in Fig. 3. The equation for the variable capacitor is as follows:

$$C_{\sim}(t) = \varepsilon \frac{A}{g - x(t)} \tag{1}$$

where $C_{\sim}(t)$ denotes the time-variable capacity, ε the dielectric constant, A the plate area, g the gap between the two plates and $x(t)$ is the corresponding mass displacement. The moving electrode of the charged capacitor results in a change of the stored electrical energy within the capacitor forcing an electrical current to flow through the external load R_{L}. The electrical output power of the energy converter is equal to the product between the current load of the external load and the corresponding voltage drop. The converted electrical energy can either be directly dissipated within an electric circuit or else be stored within an accumulator.

2.4. State space equations

Applying a straight-forward mathematical description, a basic nonlinear differential equation characterizes the mechanical and electrical part of the energy converter:

$$m\ddot{x}(t) + b_{\text{m}}\dot{x}(t) + kx(t) - F_{\text{el}}(t) = m\ddot{y}(t) \tag{2}$$

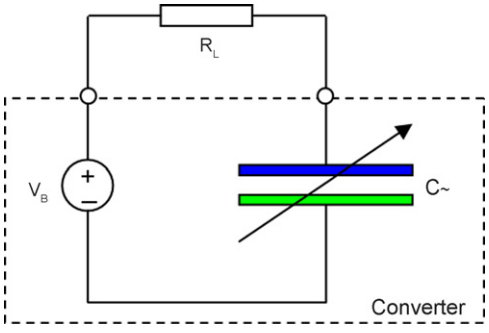

Fig. 3. Equivalent circuit diagram of the energy converter with an external load resistor R_{L}.

with

$$\ddot{y}(t) = a(t) \tag{3}$$

and

$$b_{\mathrm{m}} = \frac{m w_0}{Q_{\mathrm{m}}} \tag{4}$$

In Eqs. (2)–(4) m is the mass associated with the variable electrode, b_{m} the mechanical damping coefficient, k the spring constant, $F_{\mathrm{el}}(t)$ the electric force, $y(t)$ the displacement of the exciting source, Q_{m} the mechanical quality factor, w_0 the resonant frequency and $a(t)$ is the acceleration associated with the exciting source. The electric force is a function of the electric charge $q(t)$ according to

$$F_{\mathrm{el}}(t) = \frac{1}{2}\frac{q(t)^2}{\varepsilon A} \tag{5}$$

The time derivative of $q(t)$ corresponds to the electronic current $i(t)$ through an external load and is determined by means of the equivalent circuit diagram of Fig. 3 as follows:

$$i(t) = \dot{q}(t) = \frac{V_{\mathrm{R}}}{R_{\mathrm{L}}} = \frac{V_{\mathrm{B}} - V_C}{R_{\mathrm{L}}} = \frac{\phi_1 - \phi_2}{eR_{\mathrm{L}}} - \frac{q(t)}{C_{\sim}(t)R_{\mathrm{L}}} \tag{6}$$

where V_{R} denotes the voltage drop of the load resistance R_{L} and $V_{C_{\sim}}$ the voltage drop of the capacitor. The energy converter is completely described by the following state space equations with the three state variables namely $q(t)$, $x(t)$ and mass velocity $v(t)$:

$$\dot{q}(t) = \frac{\phi_1 - \phi_2}{eR_{\mathrm{L}}} - \frac{g - x(t)}{\varepsilon A R_{\mathrm{L}}} q(t), \qquad \dot{x}(t) = v(t),$$
$$\dot{v}(t) = -\frac{b_{\mathrm{m}}}{m} v(t) - \frac{k}{m} x(t) + \frac{1}{2m\varepsilon A} q(t)^2 + a(t) \tag{7}$$

The elementary charge is denoted as e. The output variable is defined as the electrical output power $P(t)$ of the energy converter:

$$P(t) = \frac{(\phi_1 - \phi_2)^2}{e^2 R_{\mathrm{L}}} - \frac{2(\phi_1 - \phi_2)(g - x(t))q(t)}{e\varepsilon A R_{\mathrm{L}}} + \frac{(g - x(t))^2 q(t)^2}{\varepsilon^2 A^2 R_{\mathrm{L}}} \tag{8}$$

This mathematical model based on state space equations enables the determination of optimized design parameter sets in respect to a maximum output power for a given external vibrational excitation.

3. Device simulations

3.1. Block diagram

The state space equations introduced above are transformed into a Matlab/Simulink block diagram with the objective of studying the characteristics of the capacitive energy converter. Fig. 4 presents the Matlab/Simulink block diagram.

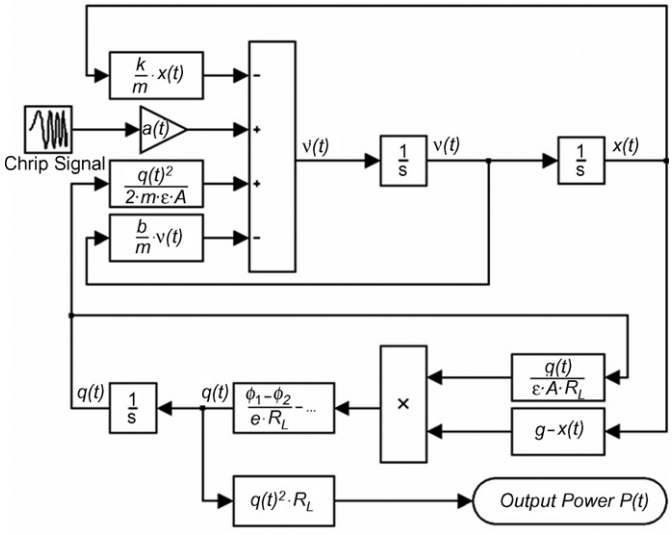

Fig. 4. Matlab/Simulink block diagram of the energy converter.

3.2. Optimum design parameter set

All following results are based on an external vibration with a frequency of 1 kHz and with an amplitude of 1.96 m/s^2 (0.2 g). Typical vibration sources are engines, turbines and industrial machines. Table 1 presents the simulation parameter set. The mass height h results from a standard thickness of a silicon-wafer (150 mm in diameter). The plate area A is limited to a reasonable MEMS die size of less than 1 cm^2. Achieving such a low mechanical damping b_{m} requires the MEMS device to be operated under low pressure.

Plate gap g and load resistance R_{L} are varied within the simulation targeting a maximum output power P. Fig. 5 displays the corresponding interdependence. Extensive numerical simulations show a maximum output power of $P = 4.28\ \mu\mathrm{W}$ at a load resistance of $R_{\mathrm{L}} = 110\ \mathrm{k}\Omega$ and a gap of $g = 4.0\ \mu\mathrm{m}$.

3.3. Electrostatic spring softening

The effect of electrostatic spring softening has already been considered within the simulations by increasing the spring constant to guarantee that the resonance frequency of the energy converter equals the external vibration frequency. This frequency matching makes sure that the converter is able to provide a maximum output power which corresponds to an optimum

Table 1
Required simulation parameter set

Simulation parameter	Symbol	Value	Unit
Plate area	A	36.00	mm^2
Mass height	h	0.675	mm
Mass density of Si	ρ	2.33	g/cm^3
Work function of Al	ϕ_1	4.08	eV
Work function of Pt	ϕ_2	6.35	eV
Mechanical damping[a]	b_{m}	4.94	g/s
Rel. permitivity (vacuum)	ε_{r}	1.00	

[a] Satisfies a mechanical quality factor of $Q_{\mathrm{m}} = 100$.

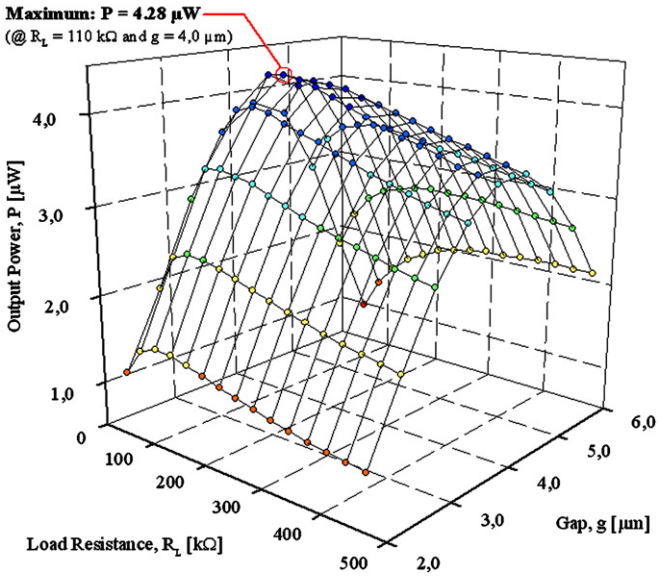

Fig. 5. Output power P vs. load resistance R_L and gap g.

efficiency. The pure mechanical spring constant for 1 kHz is determined to be $k = 2235\,\mathrm{kg/s^2}$. Fig. 6 presents the corrected spring constants depending on the load resistance at the optimum gap of 4 µm.

The optimum output power of 4.28 µW at $g = 4\,\mu\mathrm{m}$ and $R_L = 110\,\mathrm{k\Omega}$ requires an increase of the pure mechanical spring constant by 2.90% ($k_{res} = 2300\,\mathrm{kg/s^2}$). This finding is extremely important for the design of the spring geometry to operate this system in resonance.

A linearized electro-mechanical harmonic oscillator without damping effects enables to state an analytical expression for the corrected spring constant k_{res} as follows:

$$k_{res} = k + \frac{\varepsilon A(\phi_1 - \phi_2)^2}{e^2(g - x_r)^3} \approx k + \frac{\varepsilon A(\phi_1 - \phi_2)^2}{e^2 g^3} \tag{9}$$

Eq. (9) results in $k_{res} = 2261\,\mathrm{kg/s^2}$. The absolute deviation relating to k is only 39.8% of the deviation of the nonlinear model. This proves among others that a linearized model does not accurately represent the energy converter.

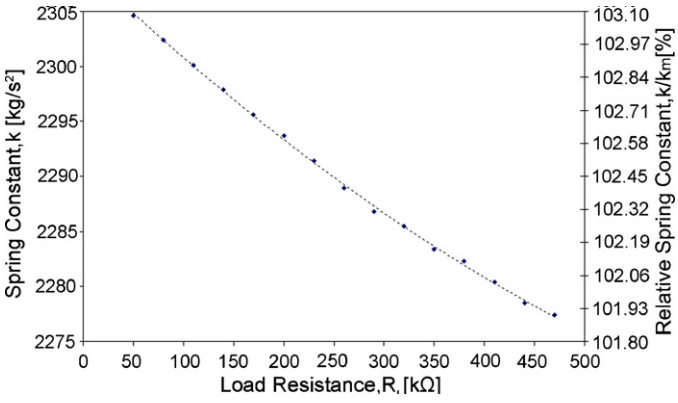

Fig. 6. Load resistance R_L vs. (relative) spring constant k.

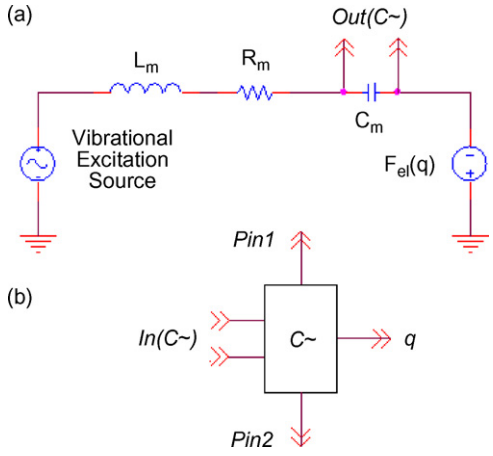

Fig. 7. PSpice model of the energy converter: (a) mechanical part and (b) variable capacitor.

4. Circuit simulations

The system of state space equations is also transformed into a PSpice model. Here, the advantage is simulating the energy converter in combination with a more complex electronic circuit. Fig. 7 presents the PSpice model of the energy converter. The model of the converter is divided into two stages. The first stage represents the equivalent circuit of the pure mechanical part of the converter (Fig. 7a). There, the damped mechanical harmonic oscillator is substituted by an equivalent electric LCR-oscillator. Here, the inertial mass is replaced by an inductance L_m, the damping coefficient by a resistor R_m and the spring constant by a capacitor C_m. The variable capacitor with its electrostatic characteristic is just indicated as a single block (Fig. 7b). Fig. 8 introduces a basic electronic circuit which stores the converted electrical energy within an external storage capacitor C_{ext}. First, the electronic output current is rectified. This rectified current charges the external capacity consequently electrical energy is stored within the storage capacitor. Further electronic stages can then be powered by this stored energy.

Fig. 9 shows the extracted electrical output power before rectification and storage. After a time of 50 ms the power becomes a maximum. Therefore, an additional circuit stage should extract the energy within the external capacitor at this time and start the loading cycle again to guarantee a high efficiency of the entire system in a real operation mode. Fig. 10 presents different elec-

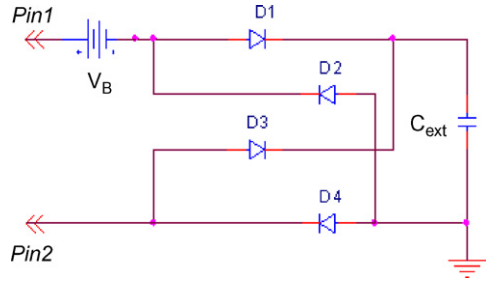

Fig. 8. Circuit for energy storage.

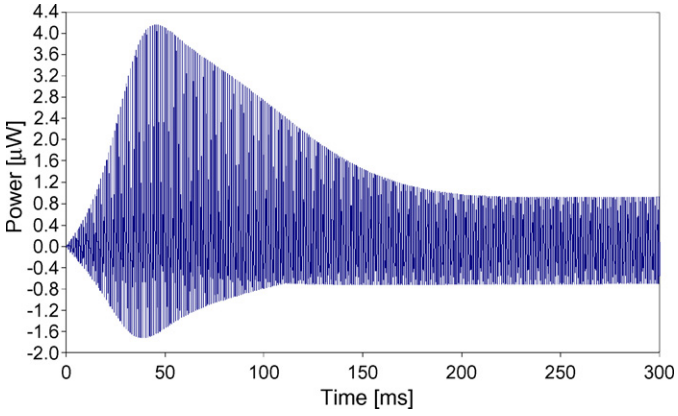

Fig. 9. Extracted power from the energy converter before rectification and storage.

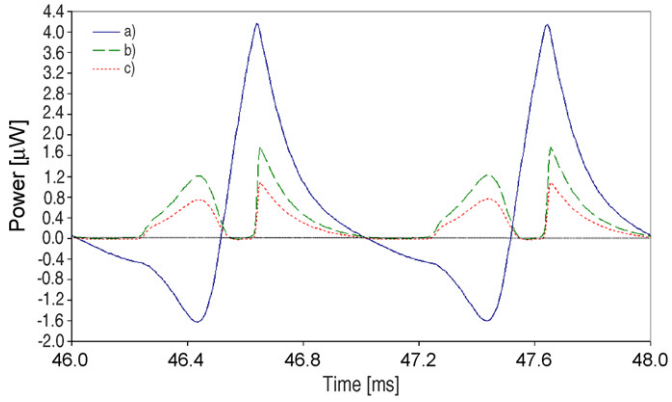

Fig. 10. Simulated electrical powers: (a) electrical power within the variable capacitor, (b) extracted power from the energy converter, and (c) available power at the external storage capacitor.

trical powers within the system for two periods of operation. The first power (Fig. 10a) is the electrical power within the electrical field of the variable capacitor, the second power (Fig. 10b) is the power that can be extracted from the capacitive energy converter and the third power (Fig. 10c) is the power which is available at the external storage capacitor. So, the electrical power that is generated within the variable capacitor is 1.1 µW in average (Fig. 10a). Consequently, the basic electronic circuit of Fig. 8 has an entire efficiency of 23% which corresponds to a power of 0.256 µW in average that can be stored within the external storage capacitor (Fig. 10c). As a next step, an appropriate electronic circuit has to be established to significantly improve the low efficiency of only 23%. There are some approaches which show that an additional dc/dc converter can maximize the transfer of energy between the capacitive converter and the energy storage circuit [18,19].

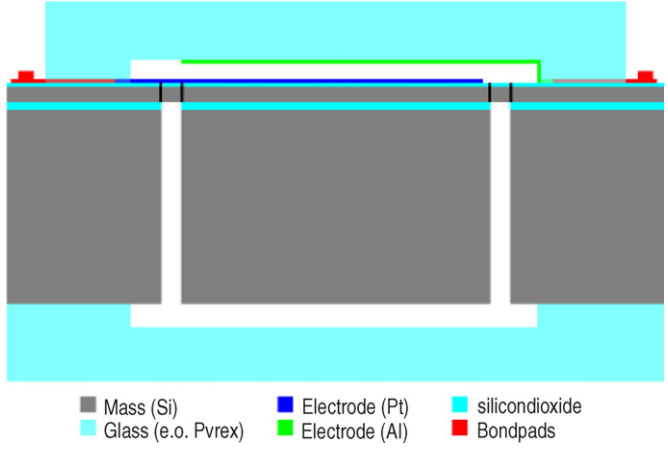

Fig. 11. Schematic cross-section of a MEMS converter.

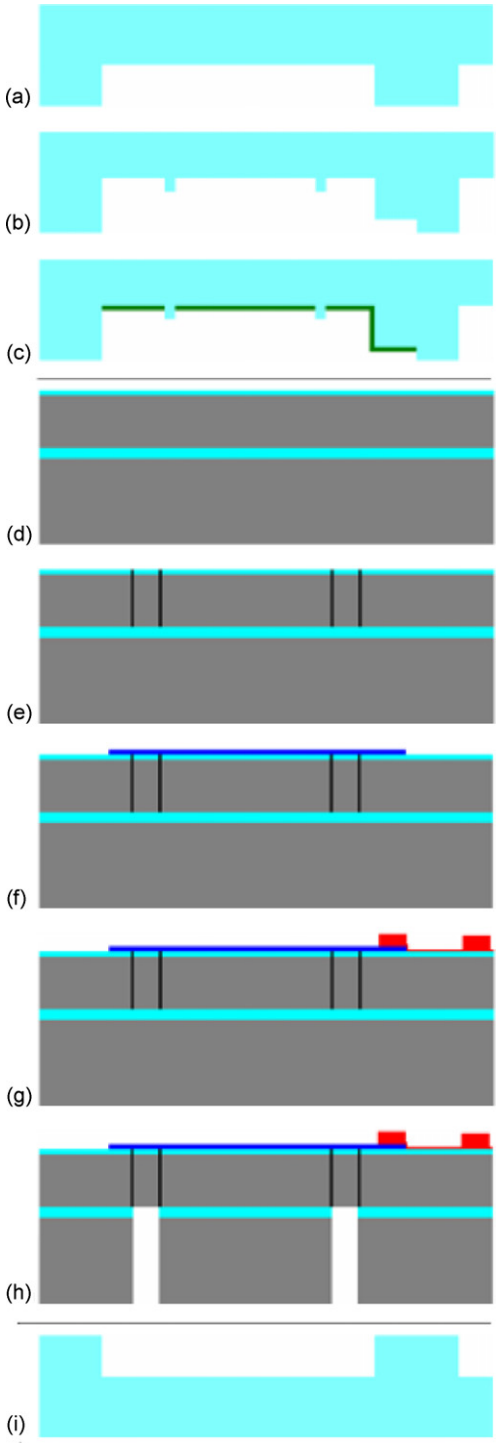

Fig. 12. Device process flow of a MEMS converter.

5. MEMS design

Fig. 11 shows a cross-section of a MEMS converter which is a device with a three wafer sandwich structure. The intermediate silicon-wafer consists of the mechanical springs, the inertial mass and the electrode. The upper glass-wafer forms the capacitor gap and the counter-electrode. The lower glass-wafer provides hermetic encapsulation and allows an operation mode under low pressure conditions. First, the upper glass-wafer is wet-etched to create the gap of the capacitor (Fig. 12a). A second wet-etch is processed in order to generate mechanical stoppers (Fig. 12b). These stoppers prevent a direct contact between electrode and counter-electrode. The etch depth is tuned in the way that the electrical force is always smaller than the mechanical elastic force to guarantee a stabile mode of operation (no electrostatic sticking). The last process step of the upper glass-wafer consists of sputtering the aluminum counter-electrode (Fig. 12c).

The surface of the intermediate SOI-wafer (Silicon-On-Insulator) is first oxidized (Fig. 12d). The springs are formed by dry-etching the upper oxidized layer and the SOI-device-layer (Fig. 12e). As a next step, the platinum electrode is sputtered (Fig. 12f). Moreover, lateral electrode feed-throughs, squeeze-contacts and bondpads are sputtered and electroplated with gold (Fig. 12g). Finally, a dry-etch from the back is performed to form and release the mass (Fig. 12h). The lower glass-wafer is simply wet-etched to enable a free movement of the mass and an encapsulation (Fig. 12i). In the end, the three wafer sandwich consisting of the upper glass-wafer, the intermediate SOI-wafer and the lower glass-wafer is anodically bonded under low pressure (Fig. 11).

6. Conclusions

This paper demonstrates a new theoretical approach to a capacitive vibration-to-electrical energy converter. The main drawback of charging the capacitor has been overcome by taking advantage of different work functions related to two different materials. As a result, a contact voltage is established between the electrodes as soon as the variable capacitor is electrically contacted, for example by an external load circuit. The contact voltage is typically in the range of a few volts (e.g. $V_B = 2.27$ V for an electrode combination of Al and Pt). The mathematical model consisting of the state space equations can easily be transformed into a Matlab/Simulink block diagram. Extensive simulations have shown that this conversion principle works. An optimum parameter set has been found for a defined external vibration if a MEMS based approach for the realization of the device is desired. The energy converter provides an maximum output power of 4.28 μW for the given vibration at a frequency of 1 kHz and an amplitude of 1.96 m/s^2 (0.2 g). The simulations have also pointed out the electrostatic spring softening which can be counteracted by a defined increase of the spring constant, ensuring that the whole system is operated in resonance and achieves a high efficiency. Moreover, a basic electronic circuit for energy storage has been modelled and simulated in PSpice. This particular circuitry has to be improved and supplemented as a next step in order to increase the efficiency of the storage module.

References

[1] F. Schmidt, Wartungsfreie Funksensoren für Gebäudetechnik, Industrie und Automobiltechnik, in: Proceedings of the Fifth Wireless Technologies Congress, Sindelfingen, Germany, 2003.
[2] J.O. Miranda, Electrostatic vibration-to-electric energy conversion, Dissertation, Massachusetts Institute of Technology at Boston, 2004.
[3] W. Cai, Vibration measurements in the switched reluctance motor, in: Proceedings of the Industry Applications Conference, Chicago, USA, 2001.
[4] M. Agah, K. Baek, J.A. Potkay, Design and Analysis of a Piezoelectric Vibration Powered MicroGenerator System, University of Michigan College of Engineering, Electrical Engineering and Computer Science, 2002.
[5] F. Lu, H.P. Lee, S.P. Lim, Modeling and analysis of micro piezoelectric power generators for micro-electromechanical-systems applications, Smart Mater. Struct. 13 (2004) 57–63.
[6] J.S. Roundy, E.S. Leland, J. Baker, E. Carleton, E. Reilly, E. Lai, Improving power output for vibration-based energy scavengers, Pervasive Comput. 4 (2005) 28–36.
[7] M.J. Ramsey, W.W. Clark, Piezoelectric energy harvesting for Bio MEMS applications, Proc. SPIE 4332 (2001) 429–438.
[8] T. Sterken, K. Baert, R. Puers, S. Borghs, Power extraction from ambient vibration, in: Proceedings of SeSens (Workshop on Semiconductor Sensors), Veldhoven, The Netherlands, 2002, pp. 680–683.
[9] F. Peano, T. Tambosso, Design and optimization of a MEMS electret-based capacitive energy scavenger, J. Micromech. Microeng. 14 (2005) 429–435.
[10] M. Mizuno, D.G. Chewtwynd, Investigation of a resonance microgenerator, J. Micromech. Microeng. 13 (2003) 209–216.
[11] M.H. Lee, C.L. Yuen, W.J. Li, H.W. Leong, Development of an AA size energy transducer with micro resonators, ISCAS'03, in: Proceedings of the International Symposium on Circuits and Systems, 2003.
[12] N.H. Ching, H.Y. Wong, W.J. Li, H.W. Leong, Z. Wen, A laser-micromachined vibrational to electrical power transducer for wireless sensing systems, in: Proceedings of the 11th International Conference on Solid-state Sensors and Actuator, Munich, Germany, 2001.
[13] C.B. Williams, C. Shearwood, M.A. Harradine, P.H. Mellor, T.S. Birch, R.B. Yates, Development of an electromagnetic micro-generator, IEE Proc. Circ. Dev. Syst. 148 (2001).
[14] J.S. Roundy, Energy scavenging for wireless sensor nodes with a focus on vibration to electricity conversion, Dissertation, University of California at Berkeley, 2003.
[15] T. Sterken, K. Baert, R. Puers, G. Borghs, R. Mertens, A new power MEMS component with variable capacitance, in: Pan Pacific Microelectronic Symposium, Hawaii, 2003, pp. 27–34.
[16] J. Arakawa, Y. Suzuki, N. Kasagi, Micro seismic power generator using electret polymer film, in: Proceedings of the Fourth International Workshop on Micro- and Nanotechnology for Power Generation and Energy Conversion Applications, Japan, 2004, pp. 187–190.
[17] P.A. Tipler, R.A. Llewellyn, Modern Physics, 3rd. ed., W.H. Freeman, New York, 1999.
[18] Y. Ammar, A. Buhrig, M. Marzencki, B. Charlot, S. Basrour, K. Matou, M. Renaudin, Wireless sensor network node with asynchronous architecture and vibration harvesting micro power generator, in: Proceedings of the Oc-EUSAI Conference, Grenoble, France, October 12–14, 2005.
[19] G. Ottmann, H. Hofmann, A. Bhatt, G. Lesieutre, Adaptive piezoelectric energy harvesting circuit for wireless remote power supply, IEEE Trans. Power Electron. 17 (2002) 669–676.

Biographies

Ingo Kuehne was born in Bautzen, Germany, in 1979. He received his diploma in engineering physics and the MEng in micro- and nanotechnology from the Munich University of Applied Sciences in 2002 and 2004, respectively. In 2004, he joined the Siemens AG Corporate Technology Department, Munich, Germany as a PhD student. His research interests are energy autonomous microsystems with emphasis on power generation and MEMS device development.

Alexander Frey was born in Jena, Germany, in 1970. He received his MA degree from the University of Texas, Austin, in 1994, and the Dipl. Phys. degree from the University of Wuerzburg, Germany in 1997. Since 1997 he has been with the Research Laboratories of Siemens AG working on the design of gigabit DRAM sensing circuits. In 1999 he joined Corporate Research, Infineon Technologies, Munich, Germany. He was engaged in the research of analog CMOS design for electrochemical sensing circuits and system related mixed signal design for biosensors. Rejoining the Research Laboratories of Siemens AG in 2005 his current interests are in the field of CMOS-based biosensors and MEMS system design.

Djordje Marinkovic was born in Belgrade, Serbia, in 1978. He received his diploma in electrical engineering from the Belgrade University in 2004. Currently, he is a postgraduate student at Belgrade University. His research interests include MEMS technology and optoelectronics.

Gerald Eckstein received his diploma degree in solid state chemistry from the University of Siegen, Siegen, Germany, in 1996, and the PhD degree in materials science from the University of Erlangen-Nuremberg, Erlangen, Germany, in 2001. He joined the Corporate Technology Department of Siemens AG, Munich, Germany, in 2001, where he has been involved in back-end processes and packaging technologies of biosensors.

Helmut Seidel was born in Munich, Germany, in 1954. He received his diploma in physics in 1980 from Ludwig-Maximilians-University in Munich, Germany. Thereafter he spent 5 years at the Fraunhofer Institute for Solid-State Technology in Munich working on his PhD, which he received in 1986 from the Free University in Berlin with a contribution on anisotropic etching of silicon. From 1986 until 2002 he held various positions in industry at MBB, Daimler Corporate Research and Temic, doing research and development on automotive sensors and microsystems. At Temic he was head of the Microsensor Development Department. Since 2002 he is professor at Saarland University in Saarbrücken, Germany, with a chair for Micromechanics, Microfluidics and Microactuators. His main interests are inertial sensors, fluidic systems and microsystems technologies. He holds more than 30 patents and has published a large number of papers. He served as Program Chairman at Transducers '01 in Munich and is member of the International Steering Committee of this Conference.